The imaging, genetic and clinical characteristics of left ventricular hypertrabeculation

Ph.D. thesis

Kinga Grebur

Semmelweis University Doctoral School
Cardiovascular Medicine and Research Division

Supervisor: Andrea Szűcs, MD, Ph.D

Official reviewers: Annamária Kosztin MD, Ph.D
Gergely Ágoston MD, Ph.D

Head of the Complex Examination Committee:
Alán Alpár MD Ph.D

Members of the Final Examination Committee:
László Cervenák MD Ph.D
Miklós Tóth MD Ph.D

Budapest
2025

1. Introduction

The healthy myocardium is formed by a compact and a trabecular layer. The trabecular meshwork is more prominent in the apex and it contributes to the electrical and mechanical function of the heart. The spectrum of normal trabeculation is wide, depending on sex, race and age, and has an individual pattern.

In recent years, the complex issue of hypertrabeculation has renewed interest, as novel recommendations entitle excessive trabeculation in otherwise healthy individuals as a normal variant. This physiological hypertrabeculation could be observed as part of cardiac adaptation in elite athletes and during pregnancy, which results from functional changes like increased preload. Pathological hypertrabeculation includes both primary form, referred to as left ventricular noncompaction (LVNC) and secondary forms associated with cardiomyopathies (CMP), congenital heart defects and extracardiac diseases.

Regarding the etiology of LVNC, mutations in genes such as TTN, MYH7, and PRDM16 play a key role in developing this morphology, and the genetic background may overlap with other CMPs. The clinical spectrum of LVNC is variable ranging from asymptomatic cases to severe complications as heart failure, arrhythmias and thromboembolic events. Imaging modalities such as cardiac magnetic resonance imaging (CMR) and echocardiography, including deformation analysis, have an important role in diagnosis, risk stratification, and clinical follow-up.

Due to the heterogenicity of clinical presentation, current guidelines advise the symptom and complication-based management of LVNC individuals with decreased cardiac function. In contrast, the recommendations are limited for LVNC individuals with preserved left ventricular ejection fraction (LVEF). Moreover, symptomatic LVNC with preserved LVEF, which could be entitled as the “grey zone” between the normal hypertrabeculated variant and LVNC with heart failure, requires clear data on genetic background, clinical manifestation and risk stratification.

2. Objectives

2.1 Different methods, different results? Threshold-based versus conventional contouring techniques in clinical practice

While both the conventional contouring (CC) and threshold-based (TB) techniques are accepted for CMR post-processing analysis, the impact of differences in trabeculated and papillary muscle mass (TPMi) on clinical diagnosis, risk stratification and therapeutic decision-making has not been investigated. Furthermore, the optimal threshold setting of the TB method is also undefined.

Therefore, our study aimed to compare left and right ventricular (LV, RV) volumetric, functional, and muscle mass parameters using CC and TB methods at 70% and 50% thresholds across various hypertrabeculated phenotypes, and to evaluate the clinical relevance of these differences.

2.2 Genetic, clinical and imaging implications of a noncompaction phenotype population with preserved ejection fraction

While the genetic background and clinical characteristics of hypertrabeculation with reduced LVEF and cardiovascular complications are well documented, limited data exist on symptomatic LVNC with preserved LVEF.

Therefore, our study aimed to characterize the genetic background and clinical presentation of symptomatic LVNC with preserved LVEF, evaluate genotype–phenotype correlations, and compare the CMR parameters with a healthy control population.

2.3 The effect of excessive trabeculation on cardiac rotation - a multimodal imaging study

Although, abnormal cardiac rotational patterns as particularly negative rigid body rotation, have been linked to LVNC, the association between cardiac rotation and genetic heterogeneity remains unexplored.

Therefore, this study aimed to assess cardiac rotation in symptomatic LVNC individuals with preserved LVEF; compare them to a healthy control population; examine the relationship between cardiac rotation, genotype and functional parameters; and evaluate the intermodality agreement between CMR and echocardiographic deformation analysis techniques.

3. Methods

3.1 Study populations

3.1.1 Different methods, different results? Threshold-based versus conventional contouring techniques in clinical practice

This retrospective CMR study included 30 individuals with dilated cardiomyopathy (DCM; 17 male, 50.7±14.7 age), 30 with arrhythmogenic cardiomyopathy (ACM; 18 male, 44.0±17.1 age), 30 with LVNC (15 male, 43.4±13.5 years) phenotype, 30 healthy athletes with >10 hours/week sports activity (15 male, 23.0±3.7 age) and 30 healthy volunteers (15 male, 37.6±11.0 age).

3.1.2 Genetic, clinical and imaging implications of a noncompaction phenotype population with preserved ejection fraction

This cross-sectional CMR study included 54 symptomatic individuals with LVNC phenotype and preserved LVEF (33 male, 39±14 age, LVEF: 65±5 %) and 54 age- and sex-matched healthy controls (33 male, 38±14 age, LVEF: 69±5 %) from a caucasian population.

3.1.3 The effect of excessive trabeculation on cardiac rotation - a multimodal imaging study

This retrospective study included 54 symptomatic individuals with an LVNC phenotype and preserved LVEF (33 male, 40.0±13.9 age, LVEF: 64.7±6.0%) and 54 age- and sex-matched healthy controls (33 male, 38.7±15.1 age, LVEF: 69.3±4.8%). All participants underwent CMR imaging, while echocardiographic assessment was performed in 39 LVNC and 40 control subjects.

3.2 CMR and echocardiographic examinations

CMR examinations were performed using 1.5 T MRI scanners (Magnetom Aera, Siemens Healthineers, Erlangen, Germany, and Achieva, Philips Medical System, Eindhoven, the Netherlands). Retrospectively gated, balanced steady-state free precession (bSSFP) cine sequences were performed with short-axis and two-, three-, and four-chamber long-axis views from base to apex, covering the whole LV and RV. Contrast agent was administered to 24 LVNC, 27 DCM, and 25 ACM patients in the first study, and to 50 LVNC individuals in the second and third studies. It was not administered to healthy volunteers or athletes.

Medis Suite software (Medis Medical Imaging Systems, Leiden, The Netherlands) was used for post-processing analysis. Manual correction of semiautomatic endocardial and epicardial contours was performed in end-diastolic and end-systolic short-axis images from base to apex. LV and RV end-diastolic (EDVi), end-systolic (ESVi), stroke volumes (SVi), EF and total myocardial mass (TMi) parameters were determined with CC and TB methods (Massk module) at 70% and 50% setups in the first study and only with TB method at 50% threshold in the second and third studies. The TPMi parameter was also measured using the TB method. All parameters were indexed to body surface area (i).

Additionally, deformation analysis was performed using the feature tracking (FT) method (QStrain module version 4.1) in the second and third studies. The short- and long-axis endocardial contours were tracked by the CMR-FT algorithm and followed throughout the cardiac cycle to determine the global longitudinal (GLS) and circumferential (GCS) strain values in the second and rotational parameters in the third study. Cardiac rotation was measured quantitatively as the endocardial end-systolic peak rotation at basal and apical levels and qualitatively as the positive (CCW) or negative (CW) direction of rotation. For the quantitative evaluation of overall cardiac rotation, the net cardiac twist parameter was calculated as the absolute difference between the apical and basal rotation. The following cardiac rotational patterns were also differentiated: normal rotation, reverse rotation, and positive and negative rigid body rotation (RBR).

In the third study, we conducted 2D transthoracic echocardiographic examinations using the GE Vivid E95 instrument with a 4Vc-D phased-array transducer (GE Vingmed Ultrasound, Horten, Norway) in 39 LVNC and 40 control individuals. ECG-gated apical two-, three- and four-chamber LA images and LV-focused parasternal SA images were acquired at the mitral valve and apical levels with a target frame rate of more than 50 frames per second. For post-processing analyses, we used the 2D Tomtec Cardiac Performance Analysis software (TOMTEC Imaging Systems GmbH, Unterschleissheim, Germany). Manually adjusted end-diastolic and end-systolic contours were applied to measure LV EDVi, ESVi, SVi values from long-axis views. The previously mentioned cardiac rotational parameters were obtained using speckle-tracking (Echo-ST) from short-axis views by tracking intramyocardial speckles throughout the cardiac cycle.

3.3 Genetic testing

Following genetic counseling, peripheral blood samples were collected from LVNC subjects for genetic analysis using next-generation sequencing with a 174-gene panel (TruSight Cardio Sequencing Kit, Illumina, USA). Variants were classified according to the American College of Medical Genetics and Genomics guidelines using databases such as Franklin, VarSome, ClinVar, ClinGen, and categorized as pathogenic (P), likely pathogenic (LP), variants of uncertain significance (VUS), likely benign, or benign. In the second study, we divided LVNC subjects based on the detected CMP-related mutations into three subgroups: the pathogenic subgroup with P or LP mutations, the VUS subgroup with VUS mutations, and the benign (B) subgroup without known relevant mutations (on 01.12.2022). CMP-related mutations were further grouped into two subtypes: directly LVNC-related when associated with "excessive trabeculation" and other CMP-related mutations. Considering the dynamic aspect of genetic information, mainly due to the reclassification of VUS mutations, the third study reclassified LVNC subgroups based on updated database information (as of 01.11.2023).

3.4 Clinical evaluation

3.4.1 Different methods, different results? Threshold-based versus conventional contouring techniques in clinical practice

When evaluating the clinical decisions using the different post-processing methods, the currently available guidelines and recommendations were applied to each patient population and athletes. The influence of using different post-processing methods to measure LV and RV parameters, the changes in clinical diagnosis, risk stratification and therapy were analyzed.

3.4.2 Genetic, clinical and imaging implications of a noncompaction phenotype population with preserved ejection fraction

Clinical data were obtained from questionnaires, during cardiogenetic counseling and from the electronic medical records. Family history assessments focused on hereditary CMP, arrhythmias and sudden cardiac death (SCD); and the personal medical history included cardiovascular symptoms (e.g., syncope, dizziness, chest pain, palpitations), arrhythmias, thromboembolic events, SCD, device implantations, known cardiac and extracardiac diseases and sport activity. To support clinical evaluation, predefined risk factors and adverse outcomes — referred to as “red flags” —

were identified based on literature. These included a positive family history of CMP or SCD, increased LVEDVi on CMR, ventricular tachycardia or fibrillation, ECG abnormalities (left bundle branch block, T-wave inversions), history of unexplained syncope, SCD or thromboembolism, nonischemic late gadollinium enhancement and an episode of minor reduction in LVEF (as low as 45%).

3.5 Statistical analysis

Statistical analyses were conducted using IBM SPSS Statistics (version 28.0, Armonk, NY). Continuous variables were reported as mean ± standard deviation or median with interquartile range, while categorical data were presented as frequencies and percentages. Normality and homogeneity of variance were assessed using the Shapiro–Wilk and Levene's tests, respectively. Group comparisons employed independent or paired t-tests, Mann–Whitney U, or Wilcoxon tests, as appropriate. For comparisons across three or more groups, ANOVA (with Tukey's post hoc), Welch's test (with Games-Howell post hoc), or Kruskal–Wallis tests were used, depending on data distribution and variance equality. Bonferroni correction was applied for multiple testing. Categorical variables were compared using chi-square or Fisher's exact tests. Pearson correlation was used for assessing associations, and multinomial logistic regression was used to analyze genotype–phenotype associations in the second study. In the third study, intermodality agreement was evaluated using the Bland-Altman analysis, and Cohen's kappa, with the chi-square test, was used to assess the strength of association regarding the direction of rotation. Interobserver reproducibility was assessed using intraclass correlation coefficients. A p-value <0.05 was considered statistically significant.

4. Results

4.1 Different methods, different results? Threshold-based versus conventional contouring techniques in clinical practice

Analyzing the trabeculation of study populations

The LVTPMi values were significantly higher in all CMP subgroups and athletes than in healthy volunteers (**Figure 1**).

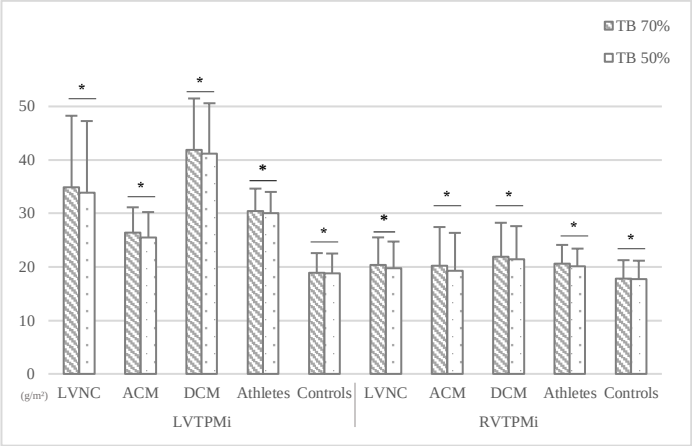

Figure 1: The LV and RV TMPi values measured with TB method at 70% and 50% thresholds,*=$p<0.05$

Comparing LV and RV parameters measured with CC and TB methods

Compared to the CC method, the TB technique with 70% and 50% setups calculated lower LV and RV volumetric and higher TMi parameters across all study groups. The LV and RV EF were significantly higher with the TB method, except for RVEF in the DCM group, where no significant difference was noted (**Table 1**).

Comparing the 70% and 50% TB thresholds

No significant differences were found in LV and RV volumetric, functional and TMi parameters between the 70% and 50% threshold settings of the TB method (**Table 1**). However, LV and RV TPMi was significantly higher at the 70% threshold compared to the 50% threshold in all study populations (**Figure 1**).

Table 1: Comparing the LV and RV parameters measured with CC technique and TB method with 70% and 50% thresholds, ¶ = p<0.05 TB method at 70% versus CC; # = p<0.05 TB 50% method versus CC.

		LV					RV				
		EDVi (ml/m²)	**ESVi** (ml/m2)	**SVi** (ml/m2)	**EF** (%)	**TMi** (g/m2)	**EDVi** (ml/m2)	**ESVi** (ml/m2)	**SVi** (ml/m2)	**EF** (%)	**TMi** (g/m2)
LVNC	**CC**	120.6 ± 32.2¶#	71.7 ± 33.0¶#	48.8 ± 8.3¶#	43.3 ± 12.9¶#	54.0 ± 15.8¶#	82.5 ± 13.9¶#	36.7 ± 9.1¶#	45.9 ± 6.5¶#	56.1 ± 5.5¶#	13.1 ± 2.2¶#
	TB 70%	86.3 ± 21.3¶	43.1 ± 21.8¶	43.2 ± 7.7¶	52.9 ± 14.9¶	90.0 ± 28.5¶	62.4 ± 10.7¶	23.5 ± 6.5¶	38.9 ± 5.6¶	62.9 ± 5.7¶	34.2 ± 6.6¶
	TB 50%	86.8 ± 21.3#	43.2 ± 21.8#	43.6 ± 7.7#	53.0 ± 14.8#	89.5 ± 28.5#	62.8 ± 10.7#	23.5 ± 6.5#	39.2 ± 5.6#	63.1 ± 5.6#	33.8 ± 6.5#
	p	*<0.001*	*<0.001*	*0.011*	*0.011*	*<0.001*	*<0.001*	*<0.001*	*<0.001*	*<0.001*	*<0.001*
ACM	**CC**	106.3 ± 15.5¶#	53.2 ± 12.9¶#	53.1 ± 10.0	50.2 ± 8.1¶#	42.9 ± 6.7¶#	121.7 ± 20.8¶#	75.8 ± 24.5¶#	47.0 ± 10.5¶#	38.8 ± 10.5¶#	19.3 ± 3.2¶#
	TB 70%	79.9 ± 12.9¶	32.3 ± 10.5¶	47.7 ± 9.5	59.9 ± 9.7¶	70.6 ± 10.6¶	101.2 ± 15.8¶	56.7 ± 22.3¶	45.5 ± 11.1¶	45.5 ± 13.5¶	40.6 ± 8.4¶
	TB 50%	80.8 ± 13.0#	32.3 ± 10.5#	48.5 ± 9.6	60.4 ± 9.6#	69.7± 10.6#	102.0 ± 15.9#	56.7 ± 22.3#	46.4 ± 11.1#	46.0± 13.4#	39.7 ± 8.2 #
	p	*<0.001*	*<0.001*	0.73	*<0.001*	*<0.001*	*<0.001*	*<0.001*	0.86	*0.01*	*<0.001*
DCM	**CC**	153.6 ± 40.9¶#	112.0 ± 37.9¶#	41.6 ± 9.0	28.3 ± 7.3¶#	71.1 ± 21.3¶#	82.9 ± 24.1¶#	39.4 ± 17.2¶#	41.3 ± 9.0¶#	52.3 ± 12.6	14.2 ± 4.1¶#
	TB 70%	111.8 ± 33.4¶	75.1 ± 29.0¶	36.7 ± 8.6	34.2 ± 7.9¶	114.9 ± 29.6¶	60.3 ± 17.2¶	25.7 ± 11.6¶	32.9 ± 8.9¶	56.8 ± 14.2	37.0 ± 9.8¶
	TB 50%	112.5 ± 33.5#	75.3 ± 29.1#	37.1 ± 8.6	34.5 ± 7.9#	114.3 ± 29.5#	60.8 ± 17.4#	25.8 ± 11.6#	33.3 ± 9.0#	56.9 ± 14.1	36.5 ± 9.7#
	p	*<0.001*	*<0.001*	0.61	*0.003*	*<0.001*	*<0.001*	*<0.001*	*<0.001*	0.332	*<0.001*
Athletes	**CC**	117.6 ± 11.1¶#	53.9 ± 7.7¶#	63.6 ± 9.8¶#	54.0 ± 5.6¶#	56.3 ± 9.0¶#	108.5 ± 12.0¶#	53.6 ± 7.3¶#	54.9 ± 8.4	50.5 ± 4.8¶#	22.5 ± 2.2¶#
	TB 70%	87.6 ± 9.6¶	31.7 ± 6.2¶	55.9 ± 9.0¶	63.7 ± 6.3¶	87.8 ± 10.8¶	88.2 ± 11.5¶	34.0 ± 5.0¶	54.3 ± 9.2	61.3 ± 4.8¶	43.6 ± 4.5¶
	TB 50%	87.8 ± 9.4#	31.8 ± 6.2#	56.0 ± 8.8#	63.7 ± 6.2#	87.2 ± 10.6#	88.7 ± 11.6#	34.3 ± 5.2#	54.5 ± 9.1#	61.2 ± 4.7#	42.7 ± 3.9#
	p	*<0.001*	*<0.001*	*0.002*	*<0.001*	*<0.001*	*<0.001*	*<0.001*	0.955	*<0.001*	*<0.001*
Healthy	**CC**	84.8 ± 12.2¶#	33.7 ± 6.7¶#	51.1 ± 8.5¶#	60.3 ± 4.9¶#	45.6 ± 7.8¶#	84.1 ± 12.3¶#	36.1 ± 8.2¶#	48.7 ± 8.9¶#	57.6 ± 6.1¶#	15.3 ± 3.5¶#
	TB 70%	65.8 ± 9.6¶	20.6 ± 4.7¶	45.2 ± 6.8¶	68.8 ± 4.7¶	65.6 ± 11.1¶	66.2 ± 10.7¶	24.9 ± 6.4¶	42.0 ± 8.7¶	62.8 ± 6.5¶	34.0 ± 5.8¶
	TB 50%	65.9 ± 9.5#	20.7 ± 4.8#	45.2 ± 6.7#	68.7 ± 4.7#	65.5 ± 11.1#	66.3 ± 10.7#	25.0 ± 6.4#	42.0 ± 8.8#	62.7 ± 6.5#	33.7 ± 5.8#
	p	*<0.001*	*<0.001*	*0.005*	*<0.001*	*<0.001*	*<0.001*	*<0.001*	*0.005*	*0.002*	*<0.001*

Analyzing the clinical impact of the CC or TB methods

Regarding the clinical impact of using different post-processing methods, we evaluated how the differences in functional and muscle mass parameters influence the diagnosis, risk stratification, and therapeutic decisions in the

studied hypertrabeculated populations. In the LVNC group, the TB method was essential for establishing the proper diagnosis through TPMi measurement and influenced additional clinical decisions in approximately 30% of individuals. In the ACM group, TB analysis influenced the evaluation of Task-Force diagnostic criteria in 67% of patients, excluded the diagnosis in 17%, reduced the need for pharmacological therapy in 33%, and not indicated ICD implantation in one case. Among DCM patients, treatment recommendations were affected in 34%, with a reduction in the estimated risk of mortality or transplantation in two individuals. Additionally, in three healthy athletes meeting both Petersen and Jacquier LVNC criteria, the TB method normalized LVEF above 50% and thus, recommended no partial sport restriction (**Table 2**).

Table 2: Modification effect of the TB method with both 70% and 50% threshold setups in clinical decision making

	What does the TB method modify?	Clinical impact	n / %
LVNC	quantification of LVTPMi	verify Jacquier diagnostic criteria	30 / 100
	reduction in LVEDVi	reduction in the risk of complications	10 / 33
	improvement in LVEF	reclassification from HFrEF to HFmrEF-pharmacotherapeutic changes	8 / 27
		reduction in the primary prophylactic criteria for anticoagulation	8 / 27
		reduction of CRT-D implantation indication	9 / 30
ACM	reduction in RVEDVi or/and improvement in RVEF	loss of ACM diagnosis	8 / 27
		loss of major Task-Force criteria	6 / 20
		reduction of major to minor Task-Force criteria	6 / 20
		loss of minor Task-Force criteria	5 / 17
	improvement in LVEF	reclassification from HFmrEF to preserved EF-pharmacotherapeutic changes	7 / 23
		reclassification from HFrEF to HFmrEF-pharmacotherapeutic changes	3 / 10
		reduction of CRT-D implantation indication	1 / 3
DCM	improvement in RVEF	reduction in the risk of mortality and cardiac transplantation	2 / 7
	improvement in LVEF	reclassification from HFrEF to HFmrEF-pharmacotherapeutic changes	5 / 17
		rejection of CRT-D implantation indication	5 / 17

Athletes	improved LVEF	falls out from partial sport restriction	3 / 10

4.2 Genetic, clinical and imaging implications of a noncompaction phenotype population with preserved ejection fraction

Genetic classification of the LVNC group

Among the LVNC group, 13 individuals (24%) were classified in the pathogenic subgroup: TTN mutations were the most frequent (46%), followed by MYH7 (15%) and others, including TNNT2, MYBPC3, MIB1, RYR2, SCN5A, and KCNQ1 (each 8%). One patient carried two pathogenic mutations in different genes (TTN and RYR2). Thirty individuals (56%) were assigned to VUS subgroup, with TTN being the most commonly affected gene (29%). Eleven individuals (20%) without known CMP-associated mutations were categorized in the benign subgroup. Further subclassification revealed that 92% of subjects in the P subgroup and 77% in the VUS subgroup harbored mutations previously linked specifically to LVNC.

Comparing the CMR parameters between the LVNC and control groups

LVNC subjects exhibited significantly elevated LV volumetric, LVTMi and LVTPMi parameters and reduced LVEF, GLS and GCS values than controls. No significant differences were found in RV parameters (**Figure 2**).

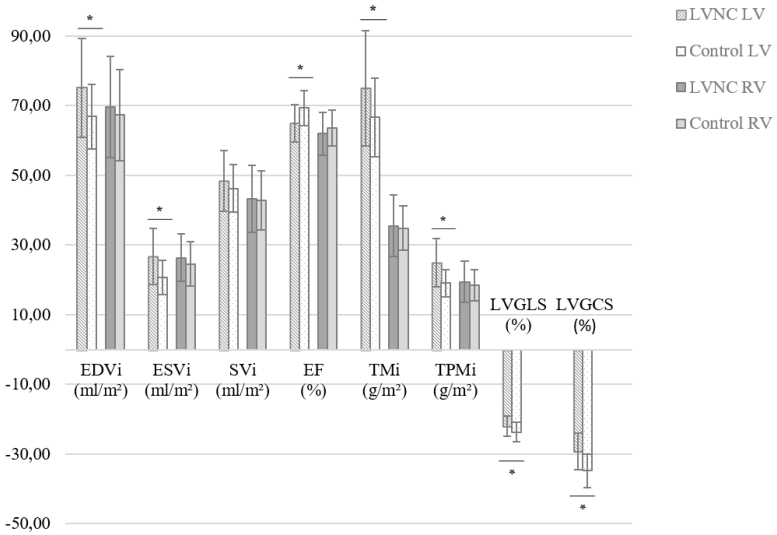

Figure 2: Comparing the LV and RV parameters between the LVNC and control groups, *=$p<0.05$

Comparing the CMR parameters among the LVNC genetic subgroups

The LV and RV functional and LV strain parameters were comparable among the genetic LVNC subgroups (**Table 3**).

Table 3: Comparing the LV and RV parameters among the three genetic subgroups

	Pathogenic (n=13)	VUS (n=30)	Benign (n=11)	p
LVEDVi	77.0 ± 15.9	75.4 ± 14.0	72.5 ± 13.5	0.748
LVESVi	26.8 ± 8.1	27.1 ± 8.4	25.9 ± 7.4	0.911
LVSVi	50.1 ± 9.8	48.3 ± 8.5	46.7 ± 7.9	0.622
LVEF	65.4 ± 5.2	64.5 ± 6.2	65.8 ± 2.6	0.758
LVTMi	75.0 ± 16.1	76.9 ± 18.0	70.0 ± 12.4	0.498
LVTPMi	26.1 ± 6.6	25.4 ± 7.9	22.7 ± 4.1	0.442
LVCMi	48.9 ± 10.7	51.5 ± 12.2	47.3 ± 10.4	0.545
RVEDVi	70.2 ± 15.9	68.9 ± 14.5	71.3 ± 14.2	0.889
RVESVi	26.3 ± 6.1	26.1 ± 7.1	27.0 ± 7.3	0.935
RVSVi	43.9 ± 11.7	42.7 ± 9.0	44.2 ± 9.7	0.874
RVEF	62.1 ± 5.9	61.9 ± 6.2	62.1 ± 7.0	0.989
RVTMi	34.8 ± 7.9	36.4 ± 10.0	34.1 ± 6.6	0.726
RVTPMi	19.4 ± 5.8	20.2 ± 6.4	17.4 ± 4.0	0.418
GLS	-21.4 ± 3.4	-22.0 ± 2.8	-22.3 ± 2.9	0.759
GCS	-29.2 ± 4.2	-28.6 ± 5.4	-30.8 ± 5.9	0.487

Analyzing the clinical characteristics of LVNC subgroups

When comparing clinical manifestations of LVNC genetic subgroups, individuals in the pathogenic and VUS categories showed a significantly higher prevalence of positive family history for CMP or SCD and a higher incidence of thromboembolic events. SCD and increased LVEDVi were observed exclusively in the pathogenic subgroup. Temporary reductions in LVEF, inverted T waves on ECG, and LGE on CMR were present in the pathogenic and VUS groups. While arrhythmias were similarly distributed across all subgroups, ventricular tachycardia appeared slightly more often in those with genetic mutations. Interestingly, atypical chest pain was significantly more common in the benign subgroup. A childhood diagnosis of LVNC was documented in 13% of the total cohort, including four in the pathogenic, two in the VUS, and one in the benign subgroup. Details are presented in **Table 4**.

Evaluating the „red flag" system

The three genetic subgroups showed significant differences in the presence and number of clinical red flags (**Figure 3**). A moderate positive correlation

was observed between genotype and red flag count and multinomial logistic regression confirmed a significant association between genotype and the red flag model ($p = 0.03$). Individuals with pathogenic directly-LVNC mutations exhibited the highest number of red flags, whereas individuals in the VUS subgroup typically presented with one to two red flags. In contrast, those in the benign subgroup had none or a single red flag.

Table 4: Comparing the clinical manifestations among LVNC genetic subgroups, *=$p<0.05$

		Genotypes of LVNC population			
		Pathogenic (n=13)	**VUS (n=30)**	**Benign (n=11)**	**p**
	Diagnosed in childhood	4	2	1	0.094
	Positive family history	8	15	1	*0.024**
Subjects' symptoms	Unexplained syncope	2	2	1	0.816
	Dizziness	6	15	8	0.355
	Atypical chest pain	5	7	8	*0.014**
	Palpitations	7	15	6	0.954
Arrhythmia	Nondocumented arrhythmia	3	5	2	0.894
	Documented arrhythmia	5	13	5	0.935
	Supraventricular arrhythmia	3	7	1	0.661
	Atrial fibrillation	0	3	1	0.638
	Ventricular arrhythmia	5	10	5	0.77
	VES	4	9	4	0.925
	Ventricular tachycardia	2	2	1	0.816
	Bradycardia	1	1	1	0.579
	AVNRT	0	2	0	0.497
Negative endpoints	Thromboembolic event	2	0	0	*0.038**
	Sudden cardiac death	1	0	0	0.201
ECG signs	T wave inversion	3	5	0	0.235
	LBBB	1	0	1	0.231
CMR parameters	↑ LVEDVi	2	0	0	0.093
	Temporary LVEF ↓	1	4	0	0.698
	LGE	2	2	0	0.671

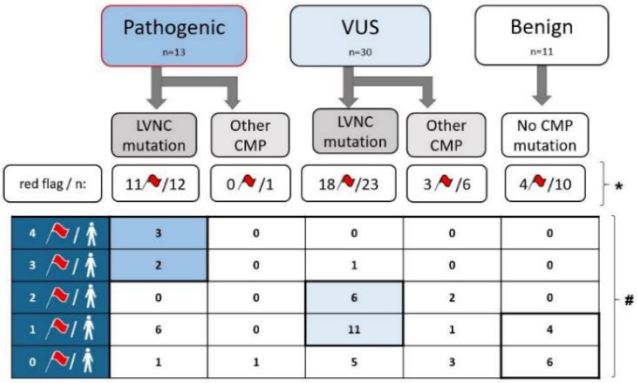

Figure 3: Evaluating the association between the red flag system and genotype, *=p < 0.05, the significance level of the chi-square test on the presence of red flags, #=p < 0.05, the significance level of the ANOVA test on the number of red flags

4.3 The effect of excessive trabeculation on cardiac rotation - a multimodal imaging study

Comparing the rotational values between the LVNC and control groups

The LVNC group showed reduced CMR-FT apical rotation and net cardiac twist in the LVNC group compared to controls. In contrast, basal rotation remained comparable between the two groups. Echo-ST analysis showed no significant differences between the groups (**Table 5**). Regarding the direction of rotation, it was similar at the basal level, whereas a negative (CW) rotation at the apical level was only observed in the LVNC group with both modalities (**Table 6**).

Comparing the cardiac rotation of the three LVNC genetic subgroups

Quantitative rotational values were comparable across the pathogenic, VUS and benign genetic subgroups (**Table 5**). In contrast, negative (CW) apical rotation was more frequent among individuals with genetic involvement; and no significant differences were observed in the direction of basal rotation between the three subgroups (**Table 6**).

Analyzing the cardiac rotational patterns

The control group exhibited a normal rotational pattern and positive RBR. Subjects in the benign subgroup predominantly showed normal rotation and positive RBR. In contrast, the VUS and pathogenic subgroups exhibited all four rotational patterns, with negative RBR present in approximately one-third to one-fourth of individuals. Additionally, reverse rotation was

identified in three cases: two pathogenic, one VUS. Results are illustrated on **Figure 4**.

Intermodality comparison of CMR-FT and Echo-ST methods

The intermodality comparison between CMR-FT and Echo-ST revealed no significant correlation or agreement for quantitative rotational values in either the LVNC or control groups (**Table 7**). However, qualitative assessments showed moderate to good agreement between the two modalities: Cohen's kappa in the LVNC group at basal 0.65, apical 0.60 and net cardiac twist 0.65, $p<0.05$; and Cohen's kappa in the control group at basal 0.40, apical 1.0, net cardiac twist 0.40, $p<0.05$.

Table 5: Comparing the rotational degrees between the LVNC and control groups and among LVNC genetic subgroups, *=p<0.05

		Control	LVNC	p	Pathogenic	VUS	Benign	p
CMR	**Basal rotation** (°)	-5.1±6.5	-3.5±7.1	0.209	-1.0±5.8	-5.0±6.7	-3.1±8.8	0.207
	Apical rotation (°)	12.3±9.3	6.7±11.0	0.005*	8.1±10.8	3.4±10.1	12.2±11.6	0.058
	Net cardiac twist (°)	17.9±10.9	12.4±9.7	0.006*	10.3±9.8	11.8±8.0	16.3±12.3	0.262
ECHO	**Basal rotation** (°)	-5.4±4.2	-5.0±6.6	0.740	-4.6±6.0	-5.8±6.4	-3.5±7.9	0.662
	Apical rotation (°)	5.7±5.0	3.8±5.5	0.106	4.9±5.3	3.6±6.5	3.0±3.0	0.769
	Net cardiac twist (°)	11.0±6.2	10.0±7.7	0.508	9.9±7.3	10.3±8.9	9.1±5.3	0.922

Table 6: Evaluating the direction of rotation among the study populations, *=p<0.05

		Control	LVNC	p	Pathogenic	VUS	Benign	p
CMR	Basal	CW:45, CCW:9	CW:40, CCW:14	0.240	CW:9, CCW:6	CW:23, CCW:4	CW:8, CCW:4	0.164
	Apical	CW:0, CCW:54	CW:15, CCW:39	0.001*	CW:5, CCW:10	CW:10, CCW:17	CW:0, CCW:12	<0.05*
ECHO	Basal	CW:38, CCW:2	CW:33, CCW:6	0.126	CW:7, CCW:2	CW:20, CCW:1	CW:6, CCW:3	0.094
	Apical	CW:0, CCW:40	CW:10, CCW:29	0.001*	CW:1, CCW:8	CW:8, CCW:13	CW:1, CCW:8	0.224

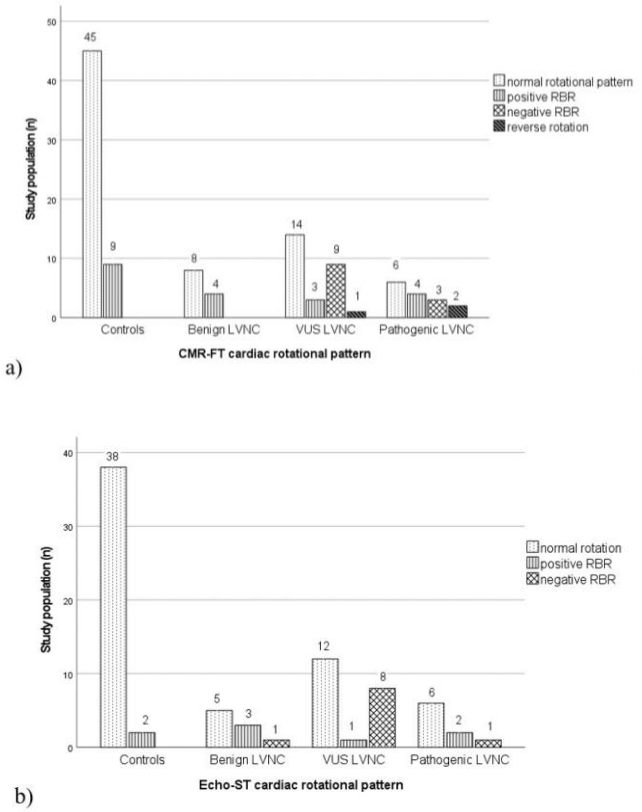

Figure 4: The distribution of cardiac rotational patterns across the control group and the three LVNC genetic subgroup with CMR-FT method (a) and Echo-ST technique (b)

Table 7: Comparing the CMR-FT and Echo-ST rotational degrees – correlations and Bland-Altman analysis

CMR-FT versus Echo-ST	Correlation		Bland-Altman analysis			
	r (p)	r (p)	Bias (p)		95% LOA	
	LVNC	C	LVNC	C	LVNC	C
Basal rotation (°)	0.33 (0.039)	-0.08 (0.626)	1.46 (0.243)	0.19 (0.884)	-13.90; 16.82	-15.91; 16.28
Apical rotation (°)	0.11 (0.496)	0.34 (0.031)	2.75 (0.179)	5.91(<0.001)	-22.37; 27.88	-10.88; 22.70
Net cardiac twist (°)	0.15 (0.366)	0.36 (0.022)	2.19 (0.239)	6.53 (<0.001)	-19.99; 24.23	-13.92; 26.97

5. Conclusions

In this thesis, we addressed the key aspects of symptomatic hypertrabeculation with preserved LVEF.

We described higher volumetric and muscle mass values and lower EF with the TB method than the CC technique. The discrepancy between the two methods influenced the assessment of diagnostic criteria, risk stratification and treatment initialization across LVNC, ACM and DCM groups and healthy athletes. Thus, TB method may be a valuable tool in excessively trabeculated individuals, particularly in borderline cases. However, updated normal values and criteria may be required for its broader application.

We identified pathogenic mutations in approximately 25% and VUS in 56% of our symptomatic hypertrabeculated population with preserved LVEF. Although CMR phenotypes were similar among the three genetic subgroups, individuals with genetic mutations exhibited a higher number of clinical red flags, underlying the relevance of genetic background in risk stratification.

We described reduced apical rotation and net cardiac twist in symptomatic LVNC with preserved LVEF compared to controls. Negative RBR was identified in a significant proportion of LVNC subjects carrying pathogenic or VUS mutations, whereas LVNC subjects from the benign subgroup and control individuals showed only normal rotation or positive RBR. Additionally, comparing the CMR-FT and Echo-ST methods the rotational pattern could serve as an early marker of functional decline in symptomatic hypertrabeculation with preserved EF.

Collectively, our results emphasize the importance of imaging modalities, genetic evaluation and clinical red flag system for a better risk stratification and management of symptomatic LVNC individuals with preserved LVEF.

6. Bibliography of the candidate's publications

Publications related to the thesis (Σ IF: 8,9):

1. **Grebur K**, Gregor Z, Kiss AR, Horváth M, Mester B, Czimbalmos C, Tóth A, Szabó LE, Dohy Z, Vágó H, Merkely B, Szűcs A. Different methods, different results? Threshold-based versus conventional contouring techniques in clinical practice. Int J Cardiol. 2023 Jun 15;381:128-134. doi: 10.1016/j.ijcard.2023.03.051. Epub 2023 Mar 23. PMID: 36965638, **IF: 3,2**.

2. **Grebur K**, Mester B, Fekete BA, Kiss AR, Gregor Z, Horváth M, Farkas-Sütő K, Csonka K, Bödör C, Merkely B, Vágó H, Szűcs A. Genetic, clinical and imaging implications of a noncompaction phenotype population with preserved ejection fraction. Front Cardiovasc Med. 2024 Feb 6;11:1337378. doi: 10.3389/fcvm.2024.1337378. PMID: 38380180; PMCID: PMC10876896, **IF: 2,8**.

3. **Grebur K**, Mester B, Horváth M, Farkas-Sütő K, Gregor Z, Kiss AR, Tóth A, Kovács A, Fábián A, Lakatos BK, Fekete BA, Csonka K, Bödör C, Merkely B, Vágó H, Szűcs A. The effect of excessive trabeculation on cardiac rotation-A multimodal imaging study. PLoS One. 2024 Sep 5;19(9):e0308035. doi: 10.1371/journal.pone.0308035. PMID: 39236040; PMCID: PMC11376564, **IF: 2,9**.

Publications not related to the thesis (Σ IF:44,352):

1. Gregor Z, Kiss AR, Szabó LE, Tóth A, **Grebur K**, Horváth M, Dohy Z, Merkely B, Vágó H, Szűcs A. Sex- and age- specific normal values of left ventricular functional and myocardial mass parameters using threshold-based trabeculae quantification. PLoS One. 2021 Oct 12;16(10):e0258362. doi: 10.1371/journal.pone.0258362. PMID: 34637474; PMCID: PMC8509873., IF: 3,752

2. Gregor Z, Kiss AR, **Grebur K**, Szabó LE, Merkely B, Vágó H, Szűcs A. MR -specific characteristics of left ventricular noncompaction and dilated cardiomyopathy. Int J Cardiol. 2022 Jul 15;359:69-75. doi: 10.1016/j.ijcard.2022.04.026. Epub 2022 Apr 15. PMID: 35436556., IF: 3,5

3. Kiss AR, Gregor Z, Popovics A, **Grebur K**, Szabó LE, Dohy Z, Kovács A, Lakatos BK, Merkely B, Vágó H, Szűcs A. Impact of Right Ventricular Trabeculation on Right Ventricular Function in Patients With Left Ventricular Non-compaction Phenotype. Front Cardiovasc Med. 2022 Apr 12;9:843952. doi: 10.3389/fcvm.2022.843952. PMID: 35498016; PMCID: PMC9041027., IF: 3,6

4. Gregor Z, Kiss AR, **Grebur K**, Dohy Z, Kovács A, Merkely B, Vágó H, Szűcs A. Characteristics of the right ventricle in left ventricular noncompaction with reduced ejection fraction in the light of dilated cardiomyopathy. PLoS One. 2023 Sep 25;18(9):e0290981. doi: 10.1371/journal.pone.0290981. PMID: 37747903; PMCID: PMC10519585., IF: 2,9

5. Horváth M, Farkas-Sütő K, Fábián A, Lakatos B, Kiss AR, **Grebur K**, Gregor Z, Mester B, Kovács A, Merkely B, Szűcs A. Highlights of right ventricular characteristics of left ventricular noncompaction using 3D echocardiography. Int J Cardiol Heart Vasc. 2023 Nov 15;49:101289. doi: 10.1016/j.ijcha.2023.101289. PMID: 38035261; PMCID: PMC10684825. , IF: 2,5

6. Ujvári A, Fábián A, Lakatos B, Tokodi M, Ladányi Z, Sydó N, Csulak E, Vágó H, Juhász V, **Grebur K**, Szűcs A, Zámodics M, Babity M, Kiss O, Merkely B, Kovács A. Right Ventricular Structure and Function in Adolescent Athletes: A 3D Echocardiographic Study. Int J Sports Med. 2024 Jun;45(6):473-480. doi: 10.1055/a-2259-2203. Epub 2024 Feb 1. PMID: 38301728; PMCID: PMC11150038., IF: 2

7. Farkas-Sütő KA, **Grebur K**, Mester B, Gyulánczi FK, Bödör C, Vágó H, Merkely B, Szűcs A. Electrocardiogram Features of Left Ventricular Excessive Trabeculation with Preserved Cardiac Function in Light of Cardiac Magnetic Resonance and Genetics. J Clin Med. 2024 Oct 3;13(19):5906. doi: 10.3390/jcm13195906. PMID: 39407966; PMCID: PMC11477278., IF: 3,0

8. Mester B, Lipták Z, Farkas-Sütő KA, **Grebur K**, Gyulánczi FK, Fábián A, Fekete BA, György TA, Bödör C, Kovács A, Merkely B, Szűcs A. Inherited Hypertrabeculation? Genetic and Clinical Insights in Blood Relatives of Genetically Affected Left Ventricular Excessive Trabeculation Patients. Life (Basel). 2025 Jan 22;15(2):150. doi: 10.3390/life15020150. PMID: 40003559; PMCID: PMC11856360., IF: 3,2

9. Horváth M, Kiss D, Márkusz I, Tokodi M, Kiss AR, Gregor Z, **Grebur K**, Farkas-Sütő K, Mester B, Gyulánczi F, Kovács A, Merkely B, Vágó H, Szűcs A. Comparison of Imaging Modalities for Left Ventricular Noncompaction Morphology. J Imaging. 2025 Jun 4;11(6):185. doi: 10.3390/jimaging11060185. PMID: 40558784; PMCID: PMC12194762, IF: 3,3

10. Horváth M, Farkas-Sütő K, Gyulánczi FK, Fábián A, Lakatos B, Kiss AR, **Grebur K**, Gregor Z, Mester B, Kovács A, Merkely B, Szűcs A. 3D Echocardiographic Assessment of Right Ventricular Involvement of Left Ventricular Hypertrabecularization from a New Perspective. J Imaging. 2025 Jun 3;11(6):181. doi: 10.3390/jimaging11060181. PMID: 40558780; PMCID: PMC12194596, IF: 3,3

11. Zamodics M, Babity M, Schay G, Bucsko-Varga A, Kovacs E, Horvath M, **Grebur K**, Laszlo MJ, Fabian A, Lakatos BK, Herczeg S, Vago H, Kovacs A, Merkely B, Kiss O. Investigation of Body Composition and Cardiac Sports Adaptation in Elite Water Polo Players. Sports (Basel). 2025 Jun 9;13(6):180. doi: 10.3390/sports13060180. PMID: 40559692; PMCID: PMC12196840, IF: 2,9

12. Mester B, Farkas-Sütő KA, Tardy JM, **Grebur K**, Horváth M, Gyulánczi FK, Vágó H, Merkely B, Szűcs A. New Solution for Segmental Assessment of Left Ventricular Wall Thickness, Using Anatomically Accurate and Highly Reproducible Automated Cardiac MRI Software. J Imaging. 2025 Oct 11;11(10):357. doi: 10.3390/jimaging11100357. PMID: 41150033; PMCID: PMC12565150, IF: 3,3

$\Sigma = 53,252$